Available online at www.sciencedirect.com
SCIENCE DIRECT
Journal of Pharmaceutical and Biomedical Analysis 41 (2006) 603–609
JOURNAL OF PHARMACEUTICAL AND BIOMEDICAL ANALYSIS
www.elsevier.com/locate/jpba

Short communication

Conformational evaluation and detailed ^{1}H and ^{13}C NMR assignments of flavoxate, a urinary tract antispasmodic agent

Nury Pérez-Hernández [a], Martha S. Morales-Ríos [b], Carlos M. Cerda-García-Rojas [b], Pedro Joseph-Nathan [b,*]

[a] *Centro de Investigación en Biología de la Reproducción, Campus Sahagún, Universidad Autónoma del Estado de Hidalgo, Apartado 1-622, Pachuca, Hidalgo 42001, Mexico*
[b] *Departamento de Química, Centro de Investigación y de Estudios Avanzados del Instituto Politécnico Nacional, Apartado 14-740, México, D.F. 07000, Mexico*

Received 2 July 2005; received in revised form 21 November 2005; accepted 22 November 2005
Available online 19 January 2006

Abstract

^{1}H and ^{13}C NMR chemical shift assignments for the urinary tract antispasmodic flavoxate (**1**) and flavoxate hydrochloride (**2**) were obtained from one- and two-dimensional measurements. A Monte Carlo random search using molecular mechanics, followed by geometry optimization of each minimum energy structure employing DFT calculations at the B3LYP/6-31G* level, and a Boltzmann analysis of the total energies, provided accurate molecular models which describe the conformational behavior of flavoxate (**1**). The electron density surfaces for the global minimum and the second minimum conformers **1a** and **1b** of this L-type Ca^{2+} channel inhibitor were calculated. The presence of both conformers in solution was demonstrated in full agreement with 2D NOESY data and NOE difference spectroscopy.

Keywords: Flavoxate; Urinary tract antispasmodic; Molecular modeling; DFT calculations; Conformational analysis; NOEDS; 2D NMR

1. Introduction

2-Piperidinoethyl 3-methylflavone-8-carboxylate or flavoxate (**1**) is supplied in pharmacy for symptomatic relief of dysuria, urgency, nocturia, suprapubic pain, prostatitis, urethritis and urethrocystitis [1]. The basic actions of the molecule are the suppression the micturition reflex [2], increment urinary bladder capacity [3] and relaxation of smooth muscle fibres of the urinary tract, through a mechanism not yet fully defined [4]. Its pharmacologic effects can be related to a direct action on the smooth muscle of the urinary tract, rather than to indirect blocking of autonomic nervous system receptors, as elicited by anticholinergic medications [5]. Flavoxate (**1**) is supplied in tablets as flavoxate hydrochloride (**2**) for oral administration; it is well absorbed from the gastrointestinal tract and rapidly metabolized producing peak blood levels in the range 0.3–0.7 μg/mL within 20 m. Tissue distribution is high in the liver, kidneys and bladder, urinary and fecal excretion is practically complete within 24 h, from which 3-methylflavone-8-carboxylic acid (MFCA) is identified as the principal metabolite.

The first synthesis of flavoxate (**1**) is reported since 1960 by acylation of 2-hydroxy-3-cyanopropiophenone with benzoyl chloride and sodium benzoate, followed by hydrolysis of the cyano group and introduction of the piperidinoethyl residue [6]. Surprisingly, there are no reports on nuclear magnetic resonance measurements of this widely used drug, in spite of the fact that thousands of flavonoids have been studied using this technique [7].

2. Experimental

2.1. General

Molecular models were generated using the MMX force field [7], as implemented in the PCMODEL program. The structures were optimized by DFT (B3LYP/6-31G*) [8] using the PCSpartan'04 program from Wavefunction (Irvine, CA, USA).

* Corresponding author. Tel.: +52 55 5747 7112; fax: +52 55 5747 7137.
E-mail address: pjoseph@nathan.cinvestav.mx (P. Joseph-Nathan).

0731-7085/$ – see front matter © 2005 Elsevier B.V. All rights reserved.
doi:10.1016/j.jpba.2005.11.042

The used tablet formulation, Bladuril® (flavoxate 200 mg as HCl salt), was purchased from a local drug store.

2.2. NMR experiments

Natural abundance ^{1}H and ^{13}C spectra were recorded on a Varian Mercury 300 spectrometer at 300 and 75.4 MHz, respectively. Spectra were referenced to TMS for ^{1}H and ^{13}C. The two-dimensional correlation experiments were performed using standard manufacturer-supplied HETCOR, gHMBC [9], NOESY and INADEQUATE [10] pulse sequences. The spectral widths in the gHMBC experiment were 18115.9 Hz for F_1 and 3597.1 Hz for F_2 and the experiment was optimized for a ^{1}J(C, H) value of 140 Hz. The INADEQUATE experiment was acquired with 1024 data points and spectral widths of 12033.7 Hz for F_2 and 6016.8 Hz for F_1, and was optimized for a ^{1}J(C, H) coupling of 150 Hz. The final signal-to-noise ratio for the INADEQUATE data was improved by use of the Full Reduction of Entire Datasets (FRED) software, available from the spectrometer manufacturer. NOESY spectra were generated with a mixing time of 0.8 s, a relaxation delay 1.0 s, data matrix 4 K × 4 K (400 increments to 4 K, zero filling in F_1, 4 K in F_2), 16 transients in each increment and a spectral width of 2801.9 Hz. In the NOE difference experiments, a pre-irradiation time of 5 s was used with the power level set at dpwr = 16 and 64 transients acquired.

2.3. Flavoxate (*1*)

A solution of flavoxate hydrochloride (500 mg) in water (3 mL) was treated with $NaHCO_3$ (100 mg). The mixture was stirred for 2 h and extracted with CH_2Cl_2 (3 mL). The organic layer was dried over Na_2SO_4 and evaporated under vacuum to yield a colorless oil. For ^{1}H and ^{13}C NMR data, see Tables 1 and 2, respectively.

2.4. Flavoxate hydrochloride (*2*)

This compound was obtained by dissolution of two BLADURIL® tablets in 5 mL of distilled water followed by filtration and washing with cold distilled water. It is a white amorphous solid. For ^{1}H and ^{13}C NMR data, see Tables 1 and 2, respectively.

3. Results and discussion

3.1. NMR measurements

A very pure sample of flavoxate (**1**) was obtained by alkaline treatment of a commercially available flavoxate-HCl (**2**) tablets formulation, as detailed in Section 2. The complete interpretation of the ^{1}H and ^{13}C NMR spectra of **1** was achieved taking into account our previous studies of flavones [11] in combination with detailed analysis of results provided by two-dimensional HETCOR, gHMBC and INADEQUATE techniques.

The ^{1}H NMR spectrum obtained from a $CDCl_3$ solution of **1** (Table 1) permitted observation of a first-order system belonging to the three A-ring protons. The H-5 and H-7 signals, whose distinction must be based on 2D heteronuclear experiments, were observed at δ 8.46 (dd, 7.8, 1.8 Hz) and 8.26 (dd, 7.5, 1.8 Hz), while the H-6 signal was observed at δ 7.44 (dd, 7.7 Hz). The ^{1}H

Table 1
^{1}H NMR data and HMBC correlations for flavoxate (**1**) and flavoxate hydrochloride (**2**)[a]

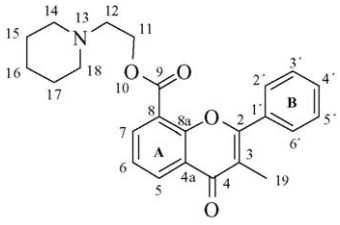

1

Hydrogen	**1**[b]	HMBC	**2**[c]
H-5	8.46 dd (7.8, 1.8)	4,7	8.33 br d (7.7)
H-6	7.44 t (7.7)	4a,7,8	7.60 t (7.7)
H-7	8.26 dd (7.5, 1.8)	5,9	8.33 br d (7.7)
CH_2-11	4.48 t (6.3)	9,12	4.54 br t (5.2)
CH_2-12	2.69 t (6.3)	11,14,18,	3.09 br m
CH_2-14,18	2.42 br t (5.1)	15,16,17	2.77 br m
CH_2-15,17	1.54 br quint (5.6)	14,16,18	1.57 br m
CH_2-16	1.41 m	14,15,17,18	1.39 br m
CH_3-19	2.24 s	2,3,4	2.10 s
H-2′,6′	7.79 m	2,4′	7.82 m
H-3′,5′	7.54 m	1′,2′,6′	7.61 m
H-4′	7.54 m	1′,2′,6′	7.61 m

[a] Multiplicities and coupling constants (in Hz) are given in parenthesis. Chemical shifts were measured at 300 MHz with TMS as internal standard.
[b] In $CDCl_3$.
[c] In DMSO-d_6.

Table 2
^{13}C NMR data of flavoxate (**1**) and flavoxate hydrochloride (**2**)[a]

Carbon	δ **1**[b]	δ **2**[c]	$W_{1/2}$ **2**	T_2*[d] **2**
C-2	161.0	160.5	1.16	1.72
C-3	117.6	117.0	1.27	1.57
C-4	178.2	177.0	1.20	1.66
C-4a	123.2	122.6	1.37	1.45
C-5	130.7	130.8	2.46	0.81
C-6	123.9	124.7	2.16	0.92
C-7	136.1	136.4	3.53	0.56
C-8	120.7	120.1	3.74	0.53
C-8a	154.4	153.8	1.52	1.31
C-9	164.3	163.3	2.69	0.74
C-11	63.1	60.8	6.24	0.32
C-12	57.1	55.2	15.37	0.13
C-14,18	54.7	53.0	8.79	0.22
C-15,17	25.8	23.6	23.38	0.08
C-16	24.0	22.1	21.57	0.09
C-19	11.7	11.5	1.56	1.28
C-1′	133.0	132.5	1.38	1.44
C-2′,6′	129.3	129.3	1.73	1.15
C-3′,5′	128.4	128.7	1.74	1.14
C-4′	130.4	130.3	3.03	0.66

[a] Chemical shifts were measured at 75.4 MHz with TMS as internal standard.
[b] In $CDCl_3$.
[c] In DMSO-d_6.
[d] Calculated from the relationship $W_{1/2} = 2/T_2^*$.

NMR signals of the five B-ring protons provide no direct information about their coupling constant values because they were observed as a strongly coupled spin–spin system. The signal at δ 7.79 (m) was assigned to the H-2′/H-6′ pair, while H-4′ and the H-3′/H-5′ pairs are overlapped at δ 7.54 (m). The methylene signals of the piperidinoethyl moiety (C-11, C-12 and C-14–C-18), and the methyl group signal C-19 were assigned to the values given in Table 1.

The ^{13}C NMR spectrum of **1**, obtained in $CDCl_3$, showed two carbonyl signals at δ 178.2 and 164.3, from which the lower field one was assigned to C-4, that in the gHMBC experiment (Fig. 1) showed correlation with the signals at δ 8.46 and 2.24 assigned to H-5 and CH_3-19, while the remaining carbonyl signal was assigned to C-9, which in the gHMBC experiment showed correlation with the signals at δ 8.26 and 4.48 assigned to H-7 and CH_2-11. The signals at δ 161.0 and 154.4 were assigned to C-2 and C-8a, respectively, which was confirmed by the gHMBC correlations with the signals at δ 7.79 (H-2′/H-6′) for C-2 and with those at δ 8.26 (H-7) and 8.46 (H-5) for C-8a. Further aromatic carbons appeared at δ 136.1, 133.0, 130.7, 130.4, 129.3, 128.4 and 123.9, which were assigned to C-7, C-1′, C-5, C-4′, C-2′/C-6′, C-3′/C-5′ and C-6, respectively, from their heteronuclear correlations.

After combined evaluation of the one-dimensional ^{1}H coupled ^{13}C NMR spectrum and the two-dimensional heteronuclear ^{1}H–^{13}C HETCOR and gHMBC spectra, the signals owing to C-4a and C-8 could not individually be assigned to the resonances at δ 120.7 and 123.2. Therefore, a two-dimensional double quantum coherence contour plot of the sp^2 spectral region of flavoxate (**1**) was obtained using the INADEQUATE pulse sequence. This experiment revealed that both signals are directly bonded to C-8a, whose signal appeared at δ 154.4. In addition, it becomes evident that the signal at δ 123.2 corresponds to C-4a since it is coupled to the keto carbonyl signal at δ 178.2 and to the C-5 signal at δ 130.7, while the signal at δ 120.7 corresponds to C-8 since it is coupled to the ester carbonyl group at δ 164.3 and to the C-7 signal at δ 136.1. In turn, both C-7 and C-5 are coupled to the C-6 signal at δ 123.9. In addition, the keto carbonyl signal at δ 178.2 is coupled to the C-3 signal at δ 117.6, which is coupled to C-2 at δ 161.0. Finally, coupling of C-2 to C-1′ at δ 133.0, of C-1′ to C-2′/C6′ at δ 129.3, of C-2′/C6′ to C3′/C5′ at δ 128.4 and of C-3′/C-5′ to C-4′ at δ 130.4 undoubtedly completes the assignment of all sp^2 carbon signal of flavoxate (**1**). The assignments of aliphatic signals corresponding to the piperinoethyl moiety of **1** are given in Table 2.

Flavoxate hydrochloride (**2**) was obtained by disolution and filtration of flavoxate-HCl tablets as indicated in Section 2. The ^{1}H NMR data of **2**, measured from a DMSO-d_6 solution, are shown in Table 1. Chemical shift assignments of **2** can be made directly by comparing their data with those of **1**, although the spectrum of **2** showed important differences as a result of protonation at the amine nitrogen atom. With the exception of the aromatic B-ring protons and methylenes CH_2-15, CH_2-16 and CH_2-17 all ^{1}H signals are shifted downfield upon protonation. The H-5 and H-7 signals appear as a sole doublet at δ 8.33 (br d, 7.7 Hz), while the H-6 signal is a triplet at δ 7.60 (t, 7.7 Hz). Resonance signals from methylenes CH_2-12, CH_2-14 and CH_2-18 in the vicinity of the amine nitrogen are broadened as well as those for CH_2-15, CH_2-16 and CH_2-17.

Comparison of the ^{1}H NMR data of **2** with that of the previously described 3-methyl-4-oxo-2-phenyl-4H-1-benzopyran-8-carboxylic acid 1,1-dimethyl-2-(*N*-piperidinyl)ethyl ester hydrochloride (terflavoxate-HCl) [12] showed good agreement in chemical shifts for all aromatic protons, with the exception of H-5 and H-7 which showed an accidental chemical shift coincidence in **2** and not in terflavoxate nor in **1**. Also, terflavoxate displayed a remarkable differentiation between the axial and equatorial hydrogen atoms of the piperidine moiety, while **1** and **2** showed averaged signals for each methylene group, evidencing a faster ring inversion of flavoxate with respect to terflavoxate.

The ^{13}C NMR spectrum of **2** showed the expected 20 signals (Table 2), from which 15 were sharp peaks. The $W_{1/2}$ values,

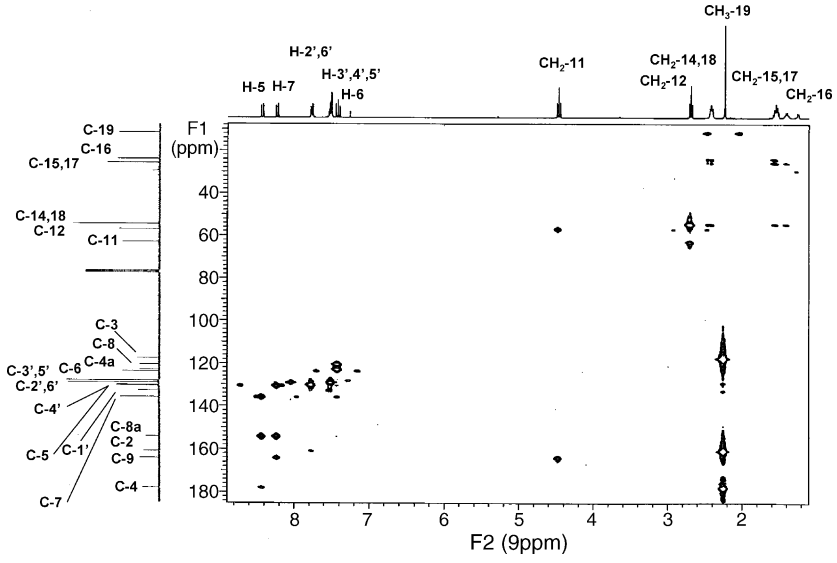

Fig. 1. gHMBC contour plot of flavoxate (**1**) in $CDCl_3$.

obtained from the full linewidths at half-height, are shown in Table 2, their corresponding T_2^* values were obtained from the $W_{1/2} = 2/T_2^*$ relationship [13]. The line broadening might be due to the presence of slow equilibria between conformations of the piperidine ring.

3.2. Conformational analysis

A theoretical conformational distribution of **1** was accomplished by means of a Monte Carlo random search [14]. A total of 79 minimum energy conformations were found within a molecular mechanics energy range of 0–6 kcal mol^{-1} (1 kcal = 4.184 kJ). A preliminary analysis of the Boltzmann distribution showed that 39 of them, within a 0–3 kcal mol^{-1} range, accounted for 97.76% of the conformational population, which evidenced the high flexibility present in **1**. In order to ascertain the conformational trajectory of **1**, the 79 structures were subjected to geometry and energy optimization by density functional theory (DFT) calculations [15,16] employing the B3LYP/6-31G* basis set. According to these calculations, the original group of 79 structures was reduced to a group of 48 because 17 conformers appeared as duplicated and 14 conformers individually account for less than 0.05% of the conformational equilibrium.

Table 3 lists the DFT energy values, the Boltzmann distribution, as well as four selected dihedral angles, which defined the molecular conformation, for the 48 most relevant conformers of **1**. Fig. 2 shows the global minimum energy conformation **1a** ($E_{DFT} = -806525.403$ kcal mol^{-1}, $E_{rel} = 0.000$ kcal mol^{-1}) and the second minimum energy conformation **1b** ($E_{DFT} = -806525.278$, $E_{rel} = 0.122$ kcal mol^{-1}), which both account for only 25.67% of the conformational equilibrium. The main difference between these two structures is the position of the piperidinoethyl moiety which is defined by the C(7)–C(8)–C(9)–O(10) dihedral angle, with values of −22.9° for **1a** and +22.2° for **1b**. The next 23 conformers account for 60.35% of the population and are classified in four groups according to the C(2′)–C(1′)–C(2)–O(1) and C(7)–C(8)–C(9)–O(10) dihedral angles.

A comparative drawing of the molecular dynamics sampling corresponding to the 23 structures plus **1a** and **1b** is depicted in Fig. 3. In the conformational groups A–D, the C(2′)–C(1′)–C(2)–O(1) dihedral angle is ca. +31.0°, −30.6°, +37.2° and −36.9°, respectively, while the C(7)–C(8)–C(9)–O(10) dihedral angle is ca. −27.1°, +23.1°, +163.2° and −165.4°, respectively. As a general fact, the DFT calculations reveal that the phenyl group adopts two main positions, which are defined by the dihedral angle C(2′)–C(1′)–C(2)–O(1), that the conformation of the piperidine ring is a chair in all conformers and that the high flexibility of **1** is due to movement of the piperidinoethyl moiety, which mainly arose from the rotation circuit of the dihedral angles C(7)–C(8)–C(9)–O(10), C(9)–O(10)–C(11)–C(12), O(10)–C(11)–C(12)–N(13) and C(11)–C(12)–N(13)–C(14). It is relevant to mention that the C(8)–C(9)–O(10)–C(11) dihedral angle remains very close to 180.0° in all conformations. According to the relative energy and Boltzmann distribution for groups A and B, it becomes evident that they represent the preferred conformations of flavoxate (**1**).

In addition, selected distances between those atoms which determine the position of the phenyl and piperidinoethyl moieties were measured in each conformer of groups A–D. In particular, minimum values were observed in structures **1a** and **1b**, as can be seen in Fig. 2. Assuming that calculated distances for those conformers can be related to experimental nuclear Overhauser effects, the corresponding NOESY spectrum was measured for **1**. Two strong correlations were observed between CH_2-11 and CH_2-14,18 and between CH_3-19 and H-2′,6′ in agreement with the measured distances of 2.18 and 2.42 Å, respectively, in the molecular models of either **1a** or **1b**. In order to obtain further information, a series of detailed NOE difference spectra was obtained for **1**. Thus, when the CH_2-11 was irradiated a 4.9% increase in the signal integral for CH_2-14,18 was observed, while irradiating CH_3-19 gave a 6.6% increase in the H-2′,6′ multiplet. Those effects were in agreement with the correlations observed in the NOESY spectrum. Furthermore, when the CH_2-11 was irradiated a NOE of 1.2% was observed for H-7. The 3.82 Å distance between H-7 and H-11 in **1b** satisfied the observed NOE effect. Finally, when CH_2-14,18 was irradiated increments of 1.2 and 1.3% were found for the integrals of H-7 and H-2′,6′, respectively, which are in agreement with distances of 3.88 Å between H-7 and H-14 in **1a** and 3.90 Å

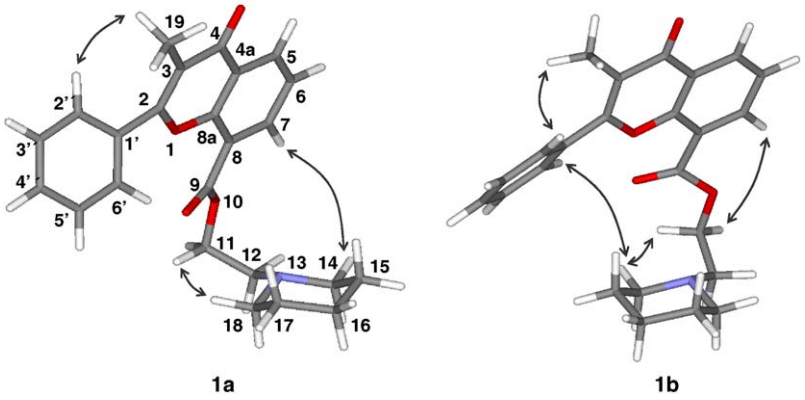

Fig. 2. Density functional theory (B3LYP/6-31G*) global minimum (**1a**) and the second minimum (**1b**) molecular models of flavoxate (**1**), showing relevant NOE correlations.

Table 3
Density functional theory (B3LYP/6-31G*) relative energy, Boltzmann distribution and four selected dihedral angles for forty eight conformers of flavoxate (**1**)

Conformer	E_{DFT}[a]	Boltzmann distribution[b]	C_7–C_8–C_9–O_{10}[c]	C_9–O_{10}–C_{11}–C_{12}[c]	O_{10}–C_{11}–C_{12}–N_{13}[c]	C_{11}–C_{12}–N_{13}–C_{14}[c]
1a[d]	0.000	14.1970	−22.9	−97.5	+61.4	−156.6
1b[d]	0.122	11.4822	+22.2	−101.5	+61.3	−158.6
1c[e]	0.601	5.1473	+158.7	−97.0	+59.3	−153.6
1d[e]	0.686	4.4540	+30.3	+82.7	+55.7	−160.3
1e[e]	0.720	4.2095	−18.1	−169.5	+179.5	−80.8
1f[e]	0.820	3.5568	−32.9	−86.9	−52.6	−67.5
1g[e]	0.837	3.4529	−21.1	−86.5	+176.1	−85.0
1h[e]	0.858	3.3322	+23.0	−87.6	−178.5	−79.5
1i[e]	0.870	3.2668	+21.4	+172.1	+82.0	−72.1
1j[e]	0.881	3.2089	−158.7	−100.4	+64.3	−158.0
1k[e]	0.891	3.1516	−22.5	+82.9	+170.1	−84.0
1l[e]	0.900	3.1049	+26.6	+89.1	+174.0	−80.3
1m[e]	0.904	3.0875	−22.7	+172.1	+176.0	−157.9
1n[e]	1.026	2.5096	+173.5	+81.3	+66.1	−151.3
1o[e]	1.113	2.1668	+159.3	−90.4	−177.4	−83.2
1p[e]	1.160	2.0032	+18.9	−177.0	+65.2	−160.7
1q[e]	1.165	1.9867	+19.5	−173.5	−85.3	−165.8
1r[e]	1.203	1.8621	−179.0	+84.8	+80.0	−73.5
1s[e]	1.245	1.7305	+167.7	+89.0	−171.0	−80.9
1t[e]	1.292	1.6022	−23.2	−87.4	−84.6	−166.7
1u[e]	1.345	1.4657	−163.9	−91.7	−68.4	−148.7
1v[e]	1.383	1.3758	+170.3	+83.2	+170.5	−85.6
1w[e]	1.417	1.2987	−168.6	+80.5	+167.7	−86.9
1x[e]	1.457	1.2127	−154.8	+87.6	+172.6	+151.8
1y[e]	1.477	1.1726	+154.3	−87.7	−172.2	−152.0
1z[f]	1.583	0.9813	−162.6	−165.1	−177.1	−77.4
1a′[f]	1.623	0.9175	+16.0	+83.7	+68.6	+62.0
1b′[f]	1.627	0.9101	+21.9	−177.0	−72.4	+71.5
1c′[f]	1.637	0.8957	−158.9	+179.5	+79.4	−76.3
1d′[f]	1.687	0.8233	+177.5	−78.9	−58.7	−76.0
1e′[f]	1.698	0.8082	+159.1	−91.4	−176.5	−83.3
1f′[f]	1.728	0.7682	−179.5	+72.3	+45.8	−165.8
1g′[f]	1.740	0.7524	−176.7	−84.8	−69.5	+70.0
1h′[f]	1.744	0.7479	−170.7	−176.7	−178.6	−84.6
1i′[f]	1.764	0.7225	−178.9	+75.3	+50.3	−163.0
1j′[f]	1.772	0.7128	−23.3	+84.4	+176.5	+66.9
1k′[f]	1.875	0.5992	−159.3	−176.3	+54.4	+174.0
1l′[f]	1.878	0.5962	+159.3	+176.7	−54.3	−48.3
1m′[f]	1.947	0.5306	+161.4	+171.6	−74.3	+69.6
1n′[f]	2.044	0.4502	+30.0	−111.8	+76.6	+60.9
1o′[f]	2.045	0.4496	−159.9	−83.3	−66.2	+73.0
1p′[f]	2.125	0.3930	−163.2	+85.1	+170.8	+66.0
1q′[f]	2.150	0.3764	+160.2	−87.4	−174.5	+67.6
1r′[f]	2.253	0.3168	−170.1	−86.7	−170.5	+66.7
1s′[f]	2.335	0.2757	−175.1	+87.5	+177.7	+67.9
1t′[f]	2.445	0.2288	+35.2	−60.9	−34.9	−71.2
1u′[f]	2.603	0.1753	+161.6	+174.5	+177.8	+64.8
1v′[f]	2.865	0.1128	+149.9	+166.0	−71.1	+73.2

[a] Density functional relative energy in kcal mol^{-1}.
[b] Expressed in percent.
[c] In degrees (°).
[d] The sum of these conformers account for 25.67% of the population.
[e] The sum of these conformers account for 60.35% of the population.
[f] The sum of these conformers account for 13.54% of the population. Dihedral angle C_8–C_9–C_{10}–O_{11} range −177.8 to +176.6°.

between H-6′ and H-18 in **1b**. Therefore, the observed NOE correlations evidenced the conformational preferences of flavoxate (**1**) in solution and validate that structures **1a** and **1b** are representative molecular models for this drug.

On the other hand, recent studies have shown that flavoxate (**1**) causes muscle relaxation through the inhibition of L-type Ca^{2+} channels in human detrusor [17]. In order to provide data which eventually could help in the elucidation of the action mechanism, we calculated the electron density surfaces at 0.08 electron/a.u.^{3} for conformers **1a** and **1b** by DFT. Fig. 4 shows the regions with less and more electron density which can interact with the receptor lipophilic sites and with calcium ions, respectively. This model can be used in the future as a template for 3D-QSAR studies.

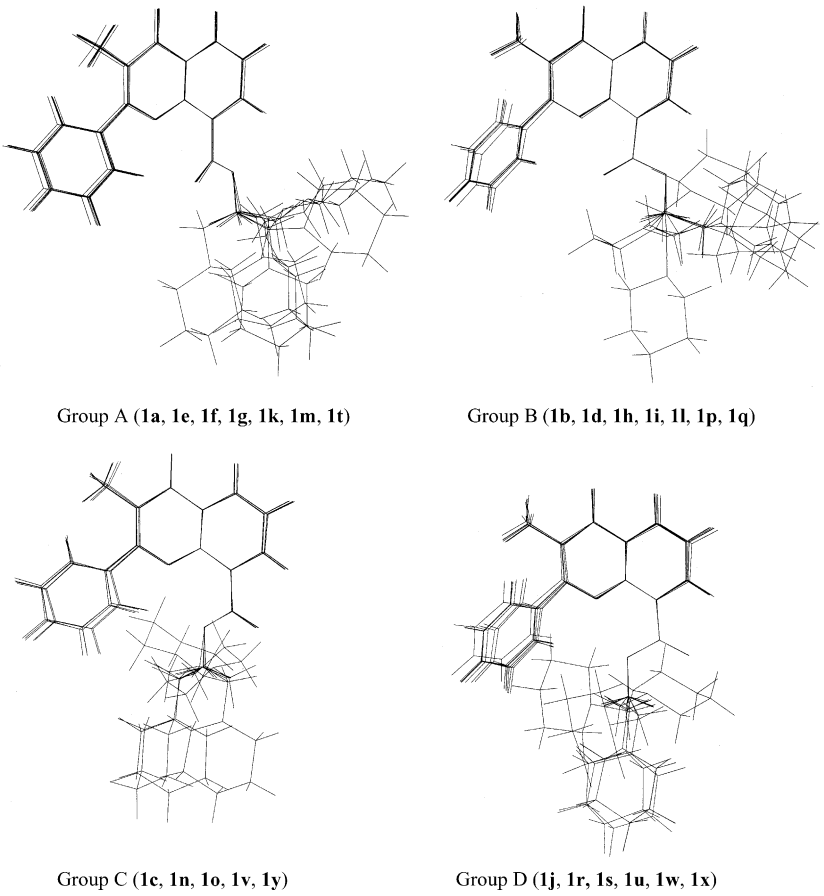

Fig. 3. Molecular dynamics samplings of four groups of conformers classified according to the value of the C(2′)–C(1′)–C(2)–O(1) and C(7)–C(8)–C(9)–O(10) dihedral angles for flavoxate (**1**).

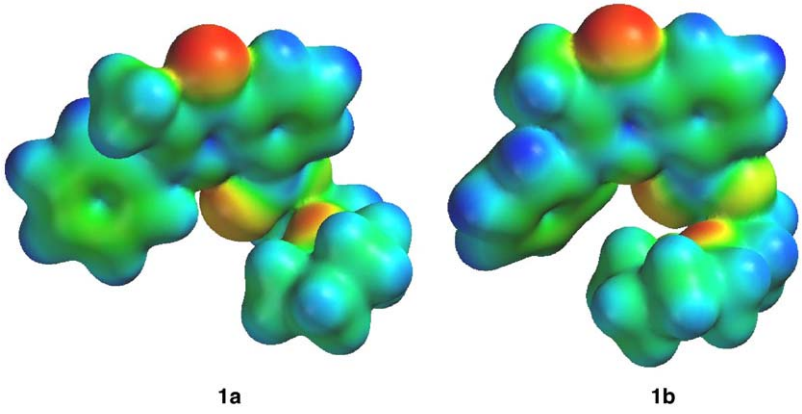

Fig. 4. Electrostatic potential surface maps for conformers **1a** and **1b** of flavoxate (**1**) obtained by DFT calculations at B3LYP/6-31G* level. The electrostatic surfaces are scaled to a range of −38 to +38 kcal/mol.

4. Conclusions

The complete structural characterization for flavoxate by NMR was made using one- and two-dimensional measurements. Conformational calculations by DFT for this compound indicate that the preferred conformations are distributed over 13 structures (groups A and B) which showed high flexibility with respect to the piperidinoethyl moiety. Furthermore, the lowest energy conformers **1a** and **1b** showed a good correlation with experimental nuclear Overhauser effects, indicating that both structures are representative molecular models for flavoxate (**1**) in solution.

References

[1] (a) G. Haeusler, H. Leitich, M. Van Trotsenburg, K. Alexandra, T. Clemens B, Obtstet. Gynecol. 100 (2002) 1003–1016;
(b) L. Guarneri, E. Robinson, R. Testa, Drugs Today 30 (1994) 91–98;
(c) R. Ruffmann, J. Int. Med. Res. 16 (1988) 317–330.

[2] (a) M. Kaseda, A. Sato, Y. Sato, Y. Torigata, Clin. Physiol. 5 (1975) 540–547;
(b) Y. Kimura, Y. Sasaki, K. Hamada, H. Fukui, Y. Ikai, Y. Yoshikuni, K. Kimura, K. Sugaya, O. Nishizawa, Int. J. Urol. 3 (1996) 218–227.

[3] E. Pedersen, Urol. Int. 32 (1977) 202–208.

[4] P. Cazzulani, R. Panzarasa, C. Luca, D. Oliva, G. Graziani, Arch. Int. Pharmacodyn. Ther. 268 (1984) 301–312.

[5] (a) S. Uckert, G.C. Stief, K.P. Odenthal, M.C. Truss, B. Lietz, U. Jonas, Arzneimittelforschung 50 (2000) 456–460;
(b) P. Cazzulani, R. Panzarasa, C. De Stefani, G. Graziani, Arch. Int. Pharmacodyn. Ther. 274 (1985) 189–200.

[6] P. Da Re, L. Verlicchi, I. Setnikar, J. Med. Chem. 2 (1960) 263–269.

[7] P.K. Agrawal, Carbon-13 NMR of Flavonoids, Elsevier, New York, 1989.

[8] U. Burket, N.L. Allinger, Molecular mechanics, in: ACS Monograph 177, American Chemical Society, Washington, DC, 1982.

[9] J. Fossey, A. Loupy, H. Strzelecka, Tetrahedron 37 (1980) 1935–1941.

[10] (a) A. Bax, M.F. Summers, J. Am. Chem. Soc. 108 (1986) 2093–2094;
(b) W. Willer, D. Leibfritz, R. Kerssebaum, W. Bermel, Magn. Reson. Chem. 31 (1993) 287–292;
(c) J. Ruiz-Cabello, G.W. Vuister, C.T.W. Moonen, P. Van-Gelderen, J.S. Cohen, P.C.M. Van- Zijl, J. Magn. Reson. 100 (1992) 282–302;
(d) A. Bax, F. Ray, T.A. Frenkiel, J. Am. Chem. Soc. 103 (1981) 2102–2104.

[11] (a) P. Joseph-Nathan, J. Mares, M.C. Hernández, J. Magn. Reson. 16 (1974) 447–453;
(b) P. Joseph-Nathan, J. Mares, D.J. Ramírez, J. Magn. Reson. 34 (1979) 57–66;
(c) P. Joseph-Nathan, D. Abramo-Bruno, M.A. Torres, Phytochemistry 20 (1981) 313–318;
(d) P. Joseph-Nathan, R.L. Santillan, Org. Magn. Reson. 22 (1984) 129–130;
(e) C. García-Martínez, M.S. Morales-Ríos, P. Joseph-Nathan, Spectroscopy 12 (1994) 85–89.

[12] A. Leonardi, R. Cappelletti, D. Nardi, F. Giordano, Arzneimittelforschung 43 (1993) 356–362.

[13] H. Günter, NMR Spectroscopy, Wiley, New York, 1980.

[14] G. Chang, W.C. Guida, W.C. Still, J. Am. Chem. Soc. 111 (1989) 4379–4386.

[15] J.P. Perdew, Phys. Rev. B 33 (1986) 8822–8824.

[16] A.D. Becke, Phys. Rev. A 38 (1988) 3098–3100.

[17] T. Tomoda, M. Aishima, N. Takano, T. Nakano, N. Seki, Y. Yonemitsu, K. Sueishi, S. Naito, Y. Ito, N. Teramoto, Br. J. Pharmacol. 146 (2005) 25–32.